CHARACTERISTICS OF A MM-WAVE TAPERED SLOT ANTENNA WITH CORRUGATED EDGES

Satoru Sugawara, Yutaka Maita, Kazuhiko Adachi, Koji Mori and Koji Mizuno*,**
General Electronics R&D Center, RICOH Company, Ltd., Natori
*Research Institute of Electrical Communication, Tohoku University, Sendai
** Photodynamics Research Center, The Institute of Physical and Chemical Research, Sendai
E-mail: sugawara@grc.ricoh.co.jp

ABSTRACT

We discuss how the radiation pattern of a reduced ground plane tapered slot antenna (TSA) is improved by varying the dimensions of a corrugated structure present at the edge of the TSA substrate. Experimental results are given that indicate that E-plane radiation patterns can be adjusted by varying the corrugation structure geometry. We also present calculated analyses of the corrugation structure using the finite-difference time-domain (FDTD) method.

INTRODUCTION

Planar antennas are desirable for many millimeter wave applications including wireless LAN communications, power combining sources, and imaging arrays for remote sensing, radio astronomy, and plasma measurement. A tapered slot antenna (TSA) is a traveling wave planar antenna that offers the advantages of wide bandwidth and high gain [1]-[4]. The slotline geometry of the TSA makes it particularly well suited for integration with uniplanar circuits.

We have previously presented two methods for improving the TSA radiation pattern [5]. First, by using the Fermi-Dirac distribution as a tapering function. Second, by using a corrugation structure around the antenna's edge (Fig. 1). Our desire has been to find a smaller TSA design that suffers no loss in performance. However, decreasing the size (i.e. ground plane width) of a TSA is known to degrade its radiation pattern [6]. In this paper we experimentally investigate how the degraded radiation patterns of reduced size TSA's can be offset through the use of corrugated edges. Results are presented that show the impact of both variations in the corrugation structure geometry, and size reductions of the antenna substrate. We also present calculated analyses of the corrugation structure using the FDTD method.

EXPERIMENTS (EFFECTS OF DIMENSIONS OF THE CORRUGATION STRUCTURE)

The corrugation structure consists of a periodic arrangement of slits at the edges of the TSA substrate. We have already reported [5] that the corrugation structure improves the radiation patterns of narrow width TSA's. However, the effects of varying the dimensions of the corrugation structure have not yet been studied. Here we investigate experimentally the effects on antenna radiation patterns by comparing several TSA's with various corrugation structure dimensions. The geometry and dimensions of the fabricated TSA's are shown in Fig.1. The Fermi antenna structure was used throughout the experiments. The antennas were fabricated on 0.05mm thick copper-clad polyimide films (Kapton (ε_r =3.5). The length L of the antennas is 20mm ($4\lambda_0$), the aperture W is 5mm (λ_0), and the distance from the aperture edge to the substrate edge d is 2.5mm ($0.5\lambda_0$). A double Y balun connects the antenna slotline to a CPW feed line and the bandwidth of this transition is greater than 15% at 60GHz (3dB). The dimensions of the slits of the corrugation structure are CW x CL, with 2CW period. The antenna patterns are measured at 60GHz. Figure 2 (a) shows the measured E-plane (filled circle) and H-plane (circle) 10dB beamwidths as a function of corrugation width (CW). The variation of the

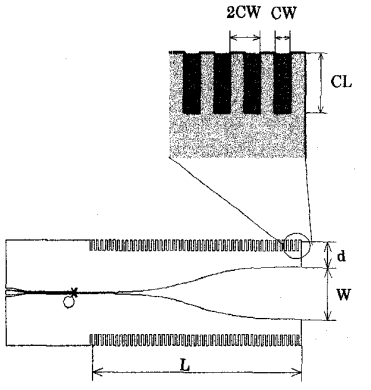

Fig.1 The geometry and dimensions of a TSA with corrugation structures (L = 20mm, W = 5mm)

0-7803-4471-5/98/$10.00 © 1998 IEEE

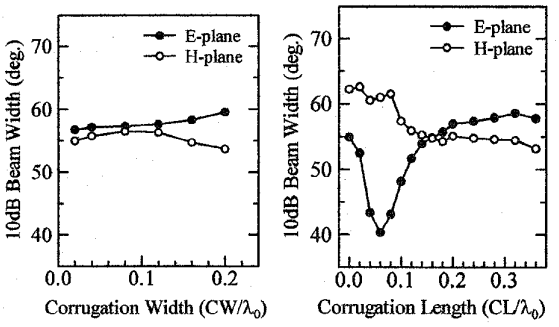

(a) Corrugation Width (b) Corrugation Length

Fig.2 The measured 10dB beam width as a function of (a) corrugation width CW(CL=$0.2\lambda_0$, d=$0.5\lambda_0$) and (b) corrugation Length CL(CW =$0.04\lambda_0$, d=$0.5\lambda_0$)

beamwidth is quite small. In Fig.2 (b) the E-plane (filled circle) and H-plane (circle) 10dB beamwidths are plotted as a function of corrugation length (CL). Only small beamwidth variations occur when increasing the corrugation length beyond $0.14\lambda_0$. However, for corrugation lengths under $0.14\lambda_0$, small changes in corrugation length dramatically impact the E-plane beamwidth. The H-plane beamwidth variations in this region are less severe. For corrugation lengths less than $0.04\lambda_0$, the corrugation structure does little to improve the radiation pattern characteristics.

EXPERIMENTS (EFFECT OF THE WIDTH OF TSA SUBSTRATE)

The effect of the total width (W + 2d in Fig. 1) of the TSA substrate on the radiation pattern has been already reported by Janaswamy [6]. Narrowing of the E-plane beamwidth is experimentally observed for decreasing the width. Similar effects were also reported by Kotthau [7] and Acharya [8]. However, because decreasing the width also involves degradation of the radiation pattern, it was difficult to investigate the effect of the substrate width extensively. The corrugation structure enables us to use a narrow width substrate without degradation of the radiation pattern [5]. This allows us to isolate the effect of the substrate width on the beamwidth. Figure 3 shows the measured E-plane (filled circle) and H-plane (circle) 10dB beamwidth as a function of substrate width (d is used as the variable, see Fig.1). In Fig.3 (a) and (b) the corrugation lengths CL are $0.08\lambda_0$ and $0.2\lambda_0$, respectively. Other parameters are the same as those in Fig.1. In both cases, as expected from the previous report, the E-plane beamwidth decreases with

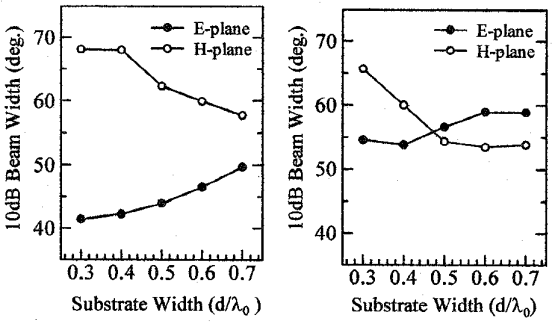

(a) CL = $0.08\lambda_0$ (b) CL = $0.2\lambda_0$

Fig.3 The measured E-plane and H-plane 10dB beam width as a function of substrate width d (CW = $0.04\lambda_0$)

narrowing width of the TSA substrate. The variation is significant for short corrugation lengths and moderate for long lengths. The H-plane beamwidth is seen to increase with narrowing width of the TSA substrate.

FDTD ANALYSES OF THE CORRUGATION STRUCTURES

The effect of the corrugation structure has been simulated using the FDTD method. The FDTD space consisted of 120 x 60 x 250 cells (Fig. 4) and used Liao's second order absorbing boundary condition. The parameters used are : dx = dz = 0.1mm (λ_0/50), dy = 0.05mm (λ_0/100) and dt = 0.1362psec. A 60GHz sinusoidal excitation was used to obtain the steady state electric field distributions. The XFDTD software (Remcom inc.) was used for this FDTD calculation. Figure 4 shows stepped approximated geometries of the Fermi antenna without corrugation (a) and with corrugation of lengths CL = $0.2\lambda_0$ (b) and CL = $0.08\lambda_0$ (c). The calculated steady state electric field is shown in Fig.5 (a), (b) and (c), respectively. Comparison between Fig.5 (a) and (b) reveals that the electric field at the edge of the antenna substrate (front and side edge) was obviously suppressed by the corrugation structure. On the other hand, higher electric field was observed at the edge of the antenna substrate in Fig.5 (c). Figure 6 shows calculated X-Y plane electric field snapshots at the front edge of the Fermi antenna without corrugation (a), and with corrugation of lengths CL = $0.2\lambda_0$ (b) and CL = $0.08\lambda_0$ (c) (Z = 240, timestep = 1200). These figures show that the direction of the electric field at the edge of the antenna substrate was also changed by the corrugation structure. In the case without corrugation, the electric field direction at the edge of the antenna substrate is opposite to the

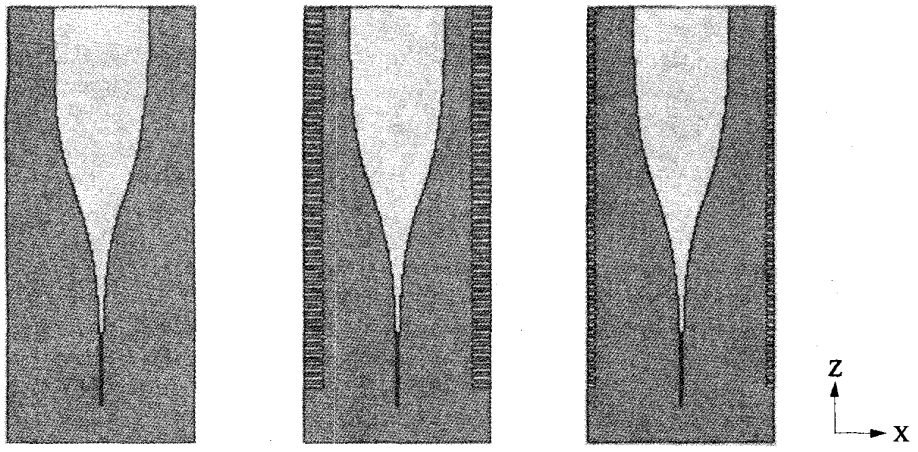

(a) without (b) with (CL = $0.2\lambda_0$) (c) with (CL = $0.08\lambda_0$)

Fig.4 Stepped approximated geometries of the Fermi antenna without corrugation (a) and with corrugation of lengths CL = $0.2\lambda_0$ (b) and CL = $0.08\lambda_0$ (c) (100 x 1 x 230 cells for each antennas)

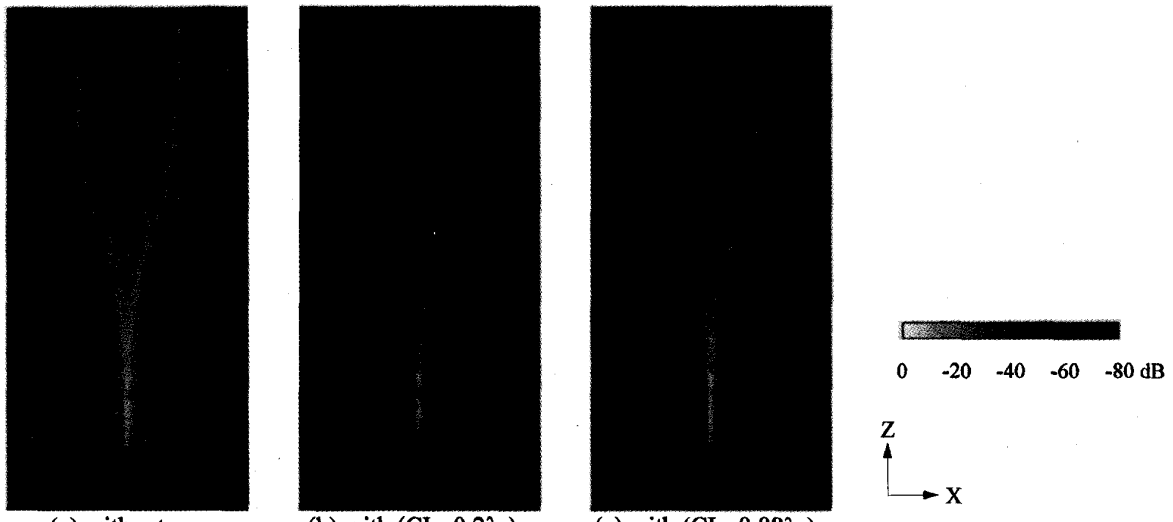

(a) without (b) with (CL=$0.2\lambda_0$) (c) with (CL=$0.08\lambda_0$)

Fig.5 The calculated steady state electric field magnitude of the Fermi antenna without corrugation (a) and with corrugation of lengths CL = $0.2\lambda_0$ (b) and CL = $0.08\lambda_0$ (c) (X-Z plane, Y = 31)

direction in the antenna aperture. In the case with corrugation, the direction at the edge is the same as the direction in the antenna aperture.

From this analysis we have made some preliminary conclusions concerning the impact of the edge corrugation. The corrugation structure alters the phase of currents flowing along the outer edge of the substrate, and changes the direction of the electric field at the edge of the antenna substrate. When the corrugation length is made longer than $0.14\lambda_0$ (or the substrate width wider), the intensity of the electric field at the edge of the antenna substrate is sufficiently suppressed, and the beamwidth ceases to be a function of corrugation length (or substrate width). When the corrugation length is made shorter than $0.14\lambda_0$ (or the substrate width narrower), the intensity of the electric field at the edge becomes stronger, increasing the effective antenna aperture, and narrowing the E-plane beamwidth. It should be noted that the corrugation width does not affect these characteristics.

CONCLUSION

We have presented detailed performance characteristics of a corrugated edge tapered slot

antenna. Experiments at 60 GHz show that E-plane radiation patterns can be adjusted by modifying the dimensions of the corrugation structure and by changing the width of the antenna substrate. We have also analyzed this TSA structure using the FDTD method. The analyses show obvious suppression of electric field intensity and change of electric field direction at the edge of the antenna substrate due to the corrugation structure. These results demonstrate that the corrugated edge TSA is very suitable for use in antenna arrays, especially for mm-wave imaging applications where short spacing between antennas is desirable.

ACKNOWLEDGMENT

The author would like to thank Prof. G. M. Rebeiz of University of Michigan for useful discussions.

REFERENCES

[1]K. S. Yngvesson, T. L. Korzeniowski, Y. S. Kim, E. L. Kollberg and J. F. Johansson, "The Tapered Slot Antenna - A New Integrated Element for MM Wave Applications", IEEE Trans. Microwave Theory and Tech., vol.37, no.2 pp.365-374, Feb. 1989.

[2] K. S. Yngvesson, D. H. Schaubert, T. L. Korzeniowski, E. L. Kollberg T. Thungren and J. F. Johansson, "Endfire Tapered Slot Antennas on Dielectric Substrates", IEEE Trans. Antennas Propagat., vol.33, no.12 pp.1392-1400, Dec. 1985.

[3] P. R. Acharya, J. Johansson, and E. L. Kollberg, "Slotline antenna for millimeter and sub millimeter wavelength," Proc. 20th Eur. Microwave Conf., Budapest, Hungary, pp353-358, Sep. 1990.

[4] P. R. Acharya, H. Ekstrom, S. S. Gearhart, S. Jacobsson, J. F. Johansson, E. L. Kollberg, G. M. Rebeiz, "Tapered Slotline Antenna at 802GHz" IEEE Trans. Microwave Theory and Tech., vol.41, no.10, pp.1715-1719, Oct. 1993.

[5] S. Sugawara, Y. Maita, K. Adachi, K. Mori and K. Mizuno, "A MM-Wave Tapered Slot Antenna with Improved Radiation Pattern", 1997 IEEE MTT-S IMS Dig., Denver, pp.959-962, 1997.

[6] Ramakrishna Janaawamy and Daniel H. Schaubert, "Analysis of the Tapered Slot Antenna" IEEE Antenna and Propagation, vol.35, no.9, pp.1058-1065, Sep. 1987.

[7] U. Kotthaus and B. Vowinknel, "Investigation of planar antennas for submillimeter receivers" IEEE Trans. Microwave Theory and Tech., vol.37, no.2 pp.375-380, Feb. 1989.

[8] P. R. Acharya, "Investigation of Slotline Antenna for Millimeter and Submillimeter Wavelengths" Tech. Rep. No. 127L, School of Elect. and Comput. Eng., Chalmers Univ. of Technol., Sweden, 1992

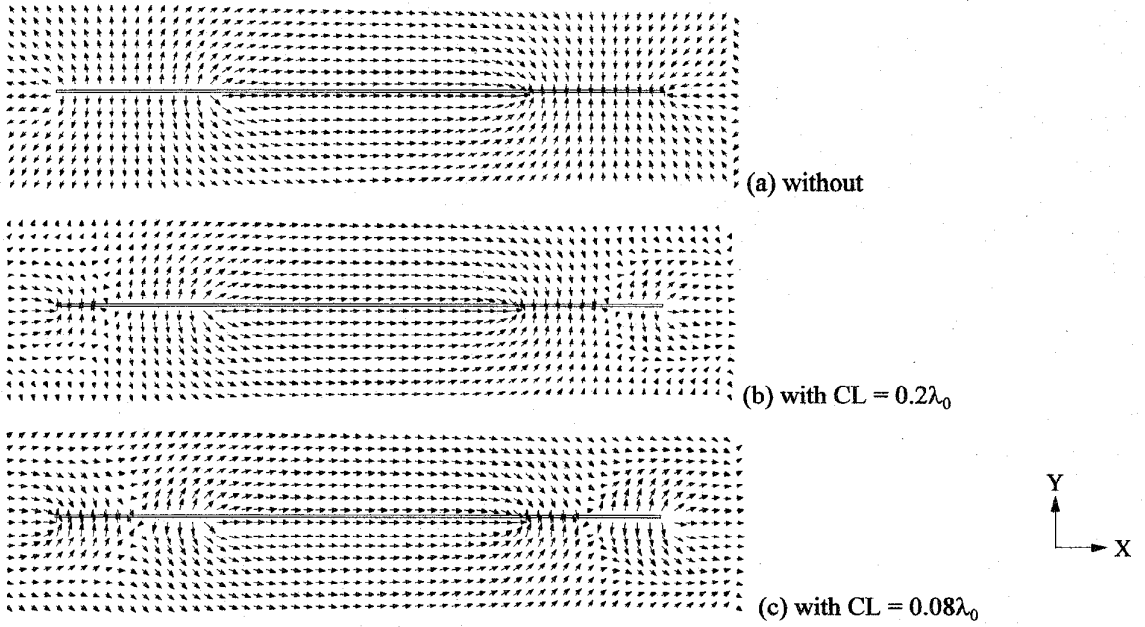

Fig.6 The calculated electric field snapshots of the Fermi antenna without (a) and with (b) CL = $0.2\lambda_0$, (c) CL = $0.08\lambda_0$ corrugation structure (X-Y plane, Z = 240 : front edge of the antenna, timestep = 1200, the solid line shows the front view of the antenna)